Interlayer closed-loop control of forming geometries for wire and arc additive manufacturing based on fuzzy-logic inference

Li, Yongzhe; Li, Xinlei; Zhang, Guangjun; Horváth, Imre; Han, Qinglin

DOI
10.1016/j.jmapro.2020.04.009

Publication date
2021

Document Version
Final published version

Published in
Journal of Manufacturing Processes

Journal of Manufacturing Processes 63 (2021) 35–47

Contents lists available at ScienceDirect

Journal of Manufacturing Processes

journal homepage: www.elsevier.com/locate/manpro

Interlayer closed-loop control of forming geometries for wire and arc additive manufacturing based on fuzzy-logic inference

Yongzhe Li [a,b], Xinlei Li [a], Guangjun Zhang [a,*], Imre Horváth [b], Qinglin Han [a]

[a] State Key Laboratory of Advanced Welding and Joining, Harbin Institute of Technology, 150001, Harbin, China
[b] Faculty of Industrial Design Engineering, Delft University of Technology, 2628 CE, Delft, the Netherlands

ARTICLE INFO

Keywords:
Wire and arc additive manufacturing
Multi-layer multi-bead deposition
Closed-loop control
Interlayer adjustment
Fuzzy-logic inference

ABSTRACT

The deposition process of wire and arc additive manufacturing (WAAM) is usually planned based on a bead geometry model (BGM), which represents the relationship between bead geometries (e.g. width, height) and required deposition parameters. However, the actual deposition situation may deviate from the one in which the BGM is built, such as varied heat dissipation conditions, resulting in morphological changes of deposited beads and geometrical errors in the formed parts. In this paper, a novel control mechanism for enhancing the fabrication accuracy of WAAM based on fuzzy-logic inference is proposed. It considers the geometrical errors measured on already deposited layers and deposition context to adjust deposition parameters of beads in the subsequent layer, forming an interlayer closed-loop control (ICLC) mechanism. This paper not only presents the theoretical fundamentals of the ICLC mechanism but also reports the technical details about utilizing this mechanism to control the forming height of multi-layer multi-bead (MLMB) components. A fuzzy-logic inference machine was applied as the core component for calculating speed change of bead deposition based on height error and previously applied change. In terms of validation, the effectiveness of the proposed control mechanism and the implemented controller was investigated through both simulative studies and real-life experiments. The fabricated cuboid blocks showed good accuracy in height with a maximum error of 0.20 mm. The experimental results implied that the proposed ICLC approach facilitates deposition continuity of WAAM, and thus enables process automation for robotic manufacturing.

1. Introduction

Wire and arc additive manufacturing (WAAM) is a promising approach for fabrication of metal parts using electric arc and feeding wire [1]. Metal inert gas (MIG), tungsten inert gas (TIG) and plasma arc (PA) are typical power sources that are employed in the existing implementations [2]. Comparing to other metal AM alternatives, such as selective laser melting [3] and electron beam melting [4], WAAM is suitable for producing parts with large-scale geometries and moderate structural complexity in a cost-competitive and time-efficient manner [5]. Solutions for enhancing the geometrical accuracy and properties of parts fabricated by WAAM have been identified as emergent topics for both academia and industry [6]. The general workflow of WAAM can be described as a sequence of procedures, including process planning, actual deposition, and post-processing [7,8]. According to the deposition manner to shape a single layer, WAAM can be classified as (i) point-by-point (PBP) deposition for building metal struts in lattice structures [9], (ii) multi-layer single-bead (MLSB) deposition for thin-walled components [10], and (iii) multi-layer multi-bead (MLMB) deposition for fabricating thick-walled (block) components [11].

The continuity of the actual WAAM process relies on predictable and repeatable depositions [12]. Concerning the geometrical aspect of a part, manufacturing parameters planned for the deposition process normally depend on a bead geometry model (BGM), which represents

Abbreviations: WAAM, wire and arc additive manufacturing; ICLC, interlayer closed-loop control; PBP, point-by-point; MLSB, multi-layer single-bead; MLMB, multi-layer multi-bead; BGM, bead geometry model; T-LOM, traditional layers-overlapping model; R-LOM, revised layers-overlapping model; MAE, mean absolute error.

* Corresponding author at: State Key Laboratory of Advanced Welding and Joining, Harbin Institute of Technology, No. 92, West Da-Zhi Street, Harbin, Heilongjiang, 150001, China.
E-mail addresses: liyongzhe87@gmail.com (Y. Li), 2432672360@qq.com (X. Li), zhanggj@hit.edu.cn (G. Zhang), I.Horvath@tudelft.nl (I. Horváth), hanqinglin2014@163.com (Q. Han).

https://doi.org/10.1016/j.jmapro.2020.04.009
Received 1 December 2019; Received in revised form 16 March 2020; Accepted 2 April 2020
Available online 24 April 2020

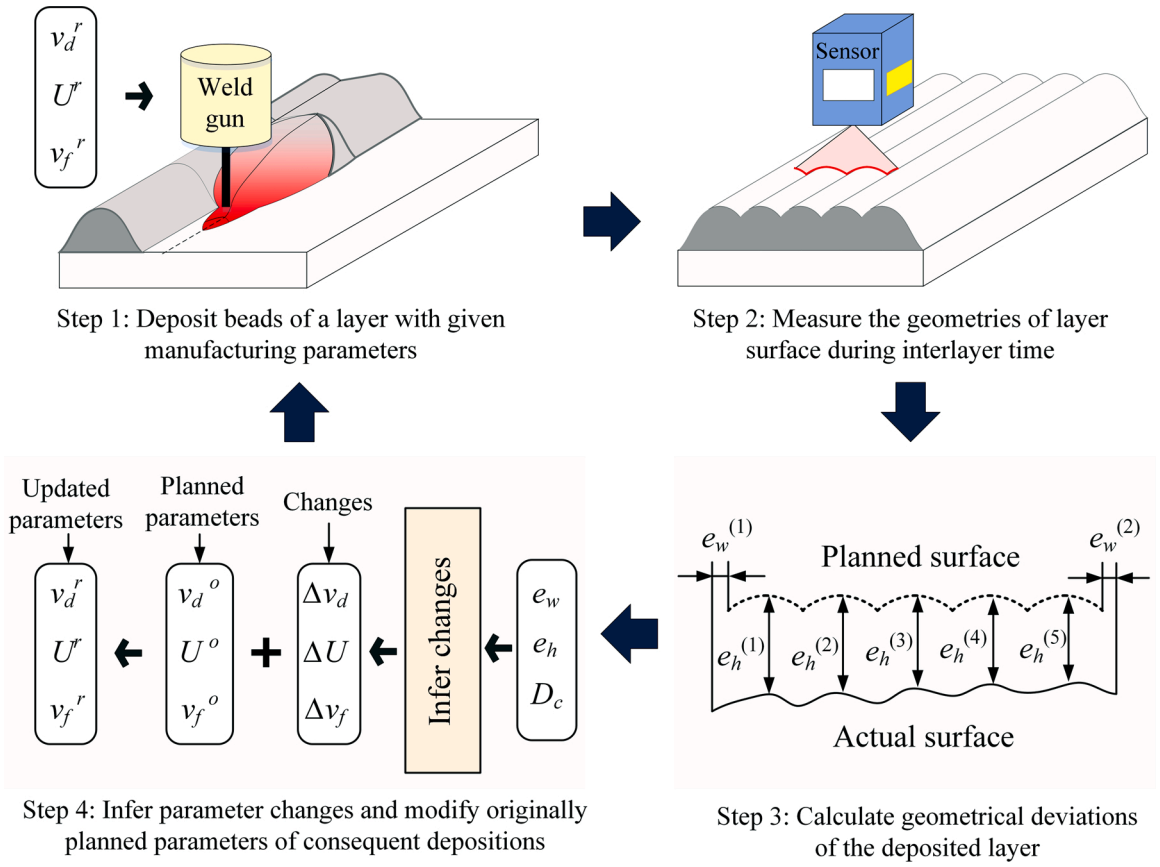

Fig. 1. General workflow of the interlayer closed-loop control mechanism for MLMB deposition.

the relationship between geometries of single weld beads (G_B) and manufacturing parameters (P_D) applied to deposit beads having G_B. In the literature, researchers usually make use of width (w_b) and height (h_b) to represent G_B [13]. Wire feed speed, voltage, and deposition speed are considered as aspects of P_D for MIG-based WAAM [14], while peak current, wire-feed speed, and travel speed are used for TIG-based WAAM [15]. However, there are many other parameters that the bead morphonology is sensitive to but have rarely been modeled mathematically, such as temperature field of weld pool, arc length, and shape of substrate. The state-of-the-art BGMs were ideally built setting these parameters as constant, such as depositing beads on a flat substrate at a given temperature with a constant nozzle height. However, there are still 5 %–10 % error rate in the reported BGMs, e.g. [14,16,17]. Observations from recent studies (e.g [18–20].) indicate that using a nominal BGM as the reference to plan parameters for the actual depositions of WAAM would result in geometrical deviations. When multiple beads and layers are overlapped, the height errors will gradually accumulate, while the width errors influence bead overlapping in MLMB cases. When the accumulated height error becomes significant, manufacturing parameters pre-planned for subsequent depositions will not be appropriate anymore and should be adjusted.

In order to improve the fabrication accuracy of WAAM, a dedicated process control strategy should be applied [21], which not only enhances stability of the deposition process [22] but also reduces material removal amount in the post-machining process [23]. To this end, many innovative approaches have been proposed by Xiong et al. to controlling the geometries of thin-wall steel parts in real-time, including a width control strategy using a learnable controller [24] and an adaptive height control solution [25]. Honnige et al. applied in-situ rolling to eliminate distortions of 2319 aluminum alloy [26]. Li et al. applied a flexible multi-point support fixture under the substrate to achieve in-process distortion control [27]. In addition, an adaptive process control scheme was proposed to solve the forming issues of corner in complex-shaped components [28]. Recently, Xu et al. proposed a feed-forward mechanism to realize the shape-driven control of deposition height on substrates with slopes [29]. The above-mentioned schemes were designed for fabrication of MLSB components, whereas other research efforts were paid for PBP depositions. For instance, to improve the dimensional accuracy of metal struts, process parameters of PBP deposition were optimized according to their influence on the geometries of built objects [9]. Radel et al. proposed an adaptive slicing strategy and a closed-loop control approach with the feedback from a camera to enhance the forming accuracy of skeleton structures [30]. It can be concluded from recent research that high geometrical accuracy has been achieved in fabrication of thin-walled and struct components. For both PBP and MLSB depositions, the temperature field of molten pool becomes stable when the layer number reaches a relatively high value [31,32]. As a result, the geometrical error of single beads converges to steady values, which enables modeling, prediction and control.

In terms of MLMB deposition, the reported work is rare. Ji et al. explored the factors that result in macro defects on block parts and reported several optimization strategies [33]. Han et al. proposed a hybrid control strategy with two closed-loop controlling subsystems to ensure the uniformity of bead width and height in MLMB structures [34]. Recent studies suggest that the accuracy of MLMB deposition is still relatively low and the surface finish of them is usually insufficient [35]. Because, MLMB deposition may experience variation of heat dissipation condition at different positions of a layer, e.g. layer edge or layer middle, which produces varied errors. Besides, due to the interactions among beads when they are overlapping, such as the spreading effect of molten pool and morphological dependency [36], the change of bead geometries not only depends on the parameters used for deposition, but also associates with some AM process-related parameters, such as the geometries of the neighboring bead(s), the deposition position in a layer

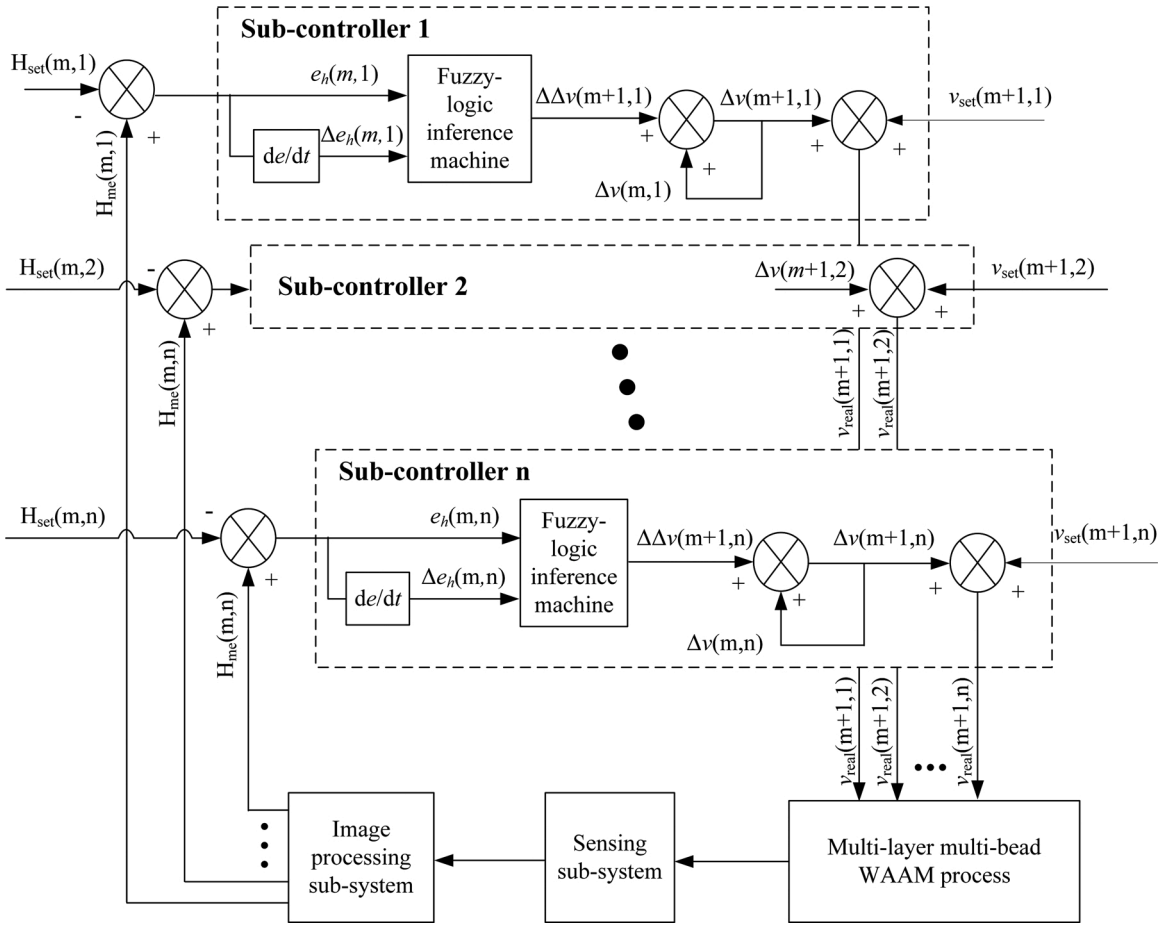

Fig. 2. Schematic diagram for controlling the forming height of multi-layer multi-bead deposition based on the ICLC mechanism.

[18], and the deposition order of beads [19]. Therefore, modeling and prediction of the geometrical errors are very complicated issues. The models and principles developed for welding process control, such as [37–40] can hardly be utilized for MLMB depositions.

The objective of this paper is to present a novel control strategy that is dedicated to MLMB deposition, namely an interlayer closed-loop control (ICLC) mechanism. Different to existing control implementations that perform parameter modifications along deposition direction, the control strategy in this paper constructs control process along vertical direction, which is perpendicular to actual depositions. Every layer is seen as a basic unit for applying a closed-loop control, and beads in a layer are individually controlled by parameter-inheritable sub-controllers. As a demonstration, this paper utilizes this mechanism for controlling the forming height of MLMB components based on a fuzzy-logic inference engine [41], which is a typical model-free approach for controlling complex welding processes [42]. Liu et al. developed an adaptive neuro-fuzzy inference system to maintain full penetration of GTAW [43]. Podržaj and Simončič showed the effectiveness of using a fuzzy logic-based controller to govern resistance spot welding processes [44]. Heidarzadeh et al. applied a fuzzy logic model to elucidate and optimize the friction stir welding of pure copper [45]. Fuzzy-logic control has also been proven as an effective approach for controlling the height of additively manufactured parts by laser depositions [46] and the width of thin-walled components by WAAM [47]. This paper presents the basic principles of the ICLC mechanism, technical details with regard to design and implementation of a fuzzy logic inference engine for MLMB depositions, and real-life case studies for the purpose of validation.

2. Mechanism of interlayer closed-loop control

2.1. Basic principles

In the process planning phase of WAAM, the motion paths and deposition parameters with regard to the entire fabrication process should be articulated concerning the CAD model of a given part, a layers-overlapping model (LOM), and a bead geometry model (BGM). The output of the process planning phase is referred to as the originally planned parameters. Due to the imperfection of the applied BGM, geometrical errors may always happen in the actual deposition processes. Accordingly, the objective of the interlayer closed-loop control (ICLC) mechanism is to ensure the geometries of deposited MLMB components to be the same as their designed values. The general workflow of the ICLC mechanism is shown in Fig. 1, which contains four operational steps in every control loop.

As the starting point, beads in a layer should be deposited using a given set of manufacturing parameters, which can be either originally planned or updated by the previous control loop. After all depositions in the layer are completed, the geometries of the layer surface are measured by a dedicated sensing operation in an off-line manner. A linear structured-light sensor can be applied to obtain the point cloud data of the layer surface, and the sampling points at selected places can be used to calculate geometrical errors between the planned surface and the formed one. In particular, the width error of a layer strongly depends on the beads formed at layer edges, whereas the height error of a layer can be represented by the height error of individual beads. As illustrated by Step 3 in Fig. 1, the width error (i.e. e_w) of a layer is defined as the deviation from the planned layer edges to the shaped ones, while the height errors (i.e. e_h) are calculated concerning the height deviation of

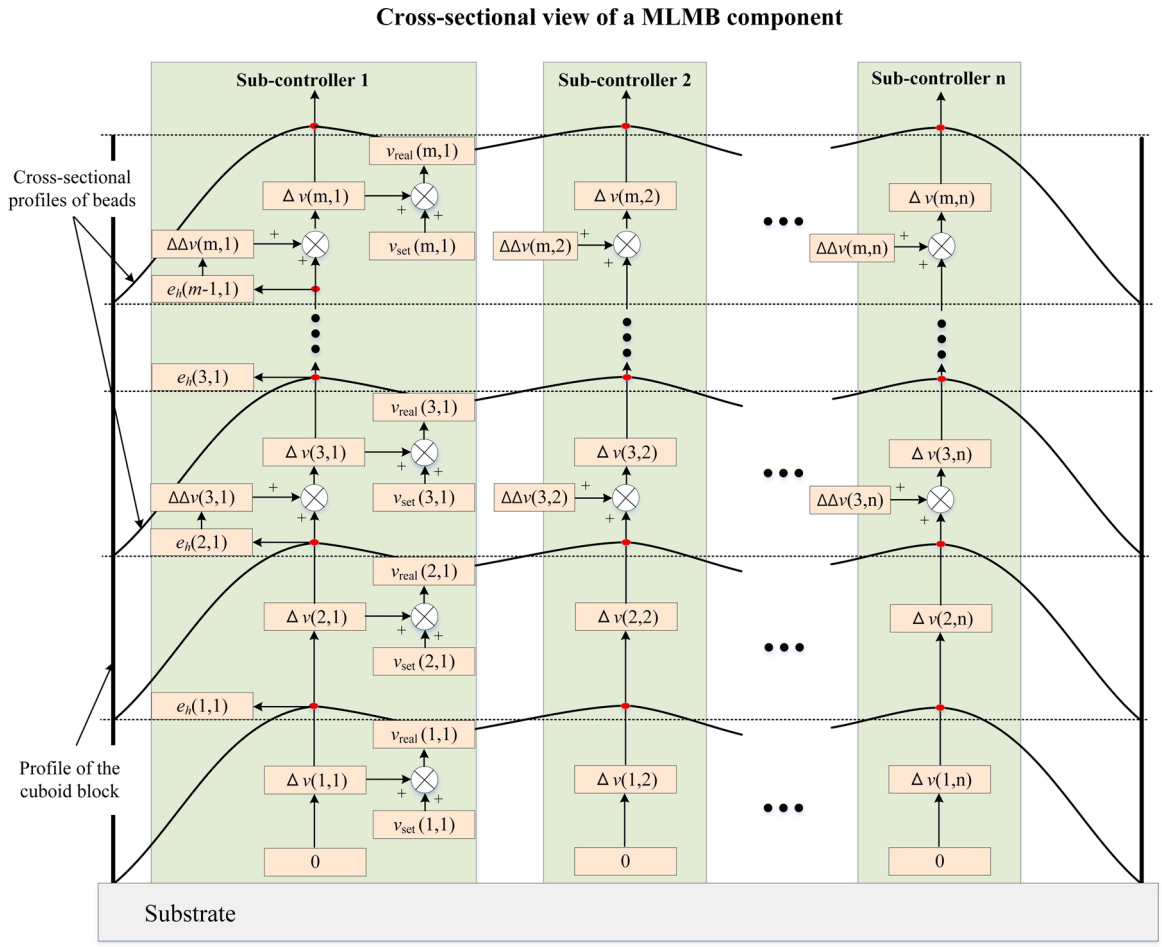

Fig. 3. Specification of the control process for fabricating a cuboid block.

beads at their deposition positions. The off-line measurement mode was used to enable applying the control strategy for complex-shaped parts, such as curved structures, corners, and intersections, in which blind areas may be experienced using on-line measurement.

Also, since multiple beads are overlapped to form a layer, the parameter adjustment should also consider the deposition context (i.e. D_c) of target beads, such as (i) the geometries of the neighbouring bead (s), which can be either in the same layer or in the support layer, (ii) the deposition position in a layer, which should distinguish the layer middle and layer edge, and (iii) the priorly applied deposition parameters and changes. All the presented factors influence the parameter adjustment for depositing a subsequent layer. They can be classified as vertical deposition context and horizontal deposition context. Fig. 1 depicts the MIG-based WAAM as an example, which employs deposition speed (v_d), deposition voltage (U), and wire-feeding rate (v_f) as deposition parameters. Changes concerning the pre-planned motion paths can also be adjusted to optimize the control process, such as application of different step-over distances between beads. For the sake of simplicity, this aspect will not be discussed in this paper.

The measured geometrical errors of the deposited layer and the deposition context of individual beads in the above layer are used to adjust the originally planned parameters for subsequent depositions. Two objectives should be achieved by the parameter adjustment. On the one hand, the updated parameters should prevent the formation of foreseeable geometrical errors in the upcoming depositions. Because, using the originally planned parameters to form the above layer will introduce new geometrical errors, resulting in error accumulation. On the other hand, the above layer to be deposited using the updated parameters should compensate for the measured deviations in height. It means that the forming height planned to be achieved by the above layer does not equal to the sliced height. After parameter changes are inferred, the updated parameters will be applied to deposit the above layer, which is also the first step of the next control loop.

According to the illustrated process, a closed-loop control mechanism is formed along the vertical direction of deposition. It considers the entire layer surface as the basic unit to adjust deposition parameters during the interlayer time. The novelty of the presented ICLC mechanism is that it allows using the deposition context (i.e. D_c) to calculate parameter changes for control. To demonstrate the effectiveness of the proposed mechanism, the ICLC mechanism has been applied in a specific control case. That is, controlling the forming height of MLMB components by adjusting the deposition speed of beads. Details will be given in the next sub-section.

2.2. *Forming height control based on the ICLC mechanism*

The forming height control approach presented in this section is dedicated to components with the same number of beads in all layers, such as cuboid blocks. Since the planned and applied deposition parameters of beads in a layer might be different, e.g. such as the process model reported by Ref. [18], beads in a layer should be individually treated. It means that the height error of beads should be individually controlled by multiple controllers. Then, the height error produced owing to a bead deposition is considered as the basis to infer speed change of the bead in the above layer in the same position. The speed change priorly applied to deposit the underneath bead is considered as the vertical deposition context to calculate a new speed change. The schematic diagram for controlling the forming height of MLMB

components based on the ICLC mechanism is shown in Fig. 2. For a component having n beads in every layer, n sub-controllers should be applied. n sets of speed change should be inferred out and applied to the originally planned parameters of the subsequent beads. Also, the interactions among neighboring beads and layers strongly influence the bead morphology in MLMB deposition, which makes it difficult to build up an accurate model to support control. For this reason, a fuzzy logic inference machine was utilized to calculate the change increments of deposition speed based on the height error and error rate.

To specify the control process of a sub-controller, $H_{set}(m, n)$ is used to represent the set height to be achieved after the n^{th} bead in the m^{th} layer is deposited. $H_{me}(m, n)$ refers to the measured height using a dedicated sensing subsystem and an image processing subsystem. Then, the height error can be noted as:

$$e_h(m,\ n)\ = H_{me}(m,\ n)\ \text{-}H_{set}(m,\ n) \tag{1}$$

The error rate, which refers to the variation of height error obtained at the same position of two successive layers, can be calculated as follows:

$$\Delta e_h(m,n)\ = e_h(m,n)\ \text{-}e_h(m\text{-}1,n) \tag{2}$$

Both error and error rate are used as inputs of the fuzzy logic inference machine, while the output is specified as the increment of a targeted speed change, $\Delta\Delta v(m+1,n)$. Accordingly, the applied speed change for depositing the bead in the above layer can be calculated by:

$$\Delta v(m+1,n)\ = \Delta v(m,n)\ + \Delta\Delta v(m+1,n) \tag{3}$$

where $\Delta\Delta v(m+1,n)$ is the increment of speed change obtained from the fuzzy-logic inference machine, $\Delta v(m,n)$ is the speed change that has been applied in the deposition of the n^{th} bead in the m^{th} layer, $\Delta v(m+1,n)$ is the speed change that will be applied to deposit the n^{th} bead in the $(m+1)^{th}$ layer. The output of a sub-controller is the real speed applied to deposit the n^{th} bead in the $(m+1)^{th}$ layer, $v_{real}(m+1,n)$, which can be obtained from the following equation:

$$v_{real}(m+1,n)\ = v_{set}(m+1,n)\ + \Delta v(m+1,n) \tag{4}$$

where $v_{set}(m+1,n)$ refers to the originally planned deposition speed of the n^{th} bead in the $(m+1)^{th}$ layer.

In the developed sub-controller, the increment of control variable change (i.e. $\Delta\Delta v$) was assigned as the output of the inference machine. This is very different from fuzzy-logic controllers for welding applications, in which the change of control variable is inferred and directly applied in a computational loop. In the steady-state of the traditional weld process control, both the error and the change of control variable are zero. On the contrary, the objective of the proposed ICLC mechanism is to find an optimal change of the control variable (i.e. an optimal Δv) applied to the predefined deposition parameters. For this reason, an increment of change (i.e. $\Delta\Delta v$) is inferred in every computational loop, and multiple increments accumulatively form the optimal change. In the steady-state of the proposed control approach, both error and error rate are zeros. Thus, the output of the fuzzy-logic inference machine (i.e. $\Delta\Delta v$) will be zero as well. It means that the previously calculated change is proven to be efficient since the applied parameters after updating lead to the achievement of the planned height. In this situation, there is no need to introduce any new increment to the previously applied change. The deposition parameters of all subsequent layers should be adjusted using the same speed change to maintain the steady-state of the control process.

According to the proposed principles, the specific control process for fabricating of a cuboid block is illustrated in Fig. 3, which is the cross-sectional view of the block. As mentioned, n sub-controllers are utilized to control the forming height of n beads. In each sub-controller, the speed change (i.e. Δv) is defined as a variable that should be inherited over the entire fabrication process. The initial value of Δv in all sub-controllers is specified as 0, which assumes that the originally planned speeds are appropriate for depositions. According to Eq. (2), the error rate is calculated using the height information of two successive layers. For this reason, beads in the first two layers should be deposited with the originally planned parameters before adjustments can be made. Thus, the following initial conditions of the control process can be set:

$$\Delta v(1,\ i) = 0 \text{and } \Delta v(2,i) = 0 \tag{5}$$

$$v_{set}(1,\ i) = v_{real}(1,\ i) v_{set} \text{ and } v_{set}(2,\ i) = v_{real}(2,\ i) \tag{6}$$

where $i = 1,\ 2,\ \ldots, n$. After the second layer is deposited, the measured $e_h(1,i)$ and $e_h(2,i)$ are used to infer $\Delta\Delta v(3,i)$. Then, $\Delta v(3,i)$ can be revised taking $\Delta\Delta v(3,i)$ into consideration. The calculated $\Delta v(3,i)$ is further utilized to update $v_{set}(3,i)$, predicting that the obtained $v_{real}(3,i)$ will properly eliminate the produced error in height. After the actual depositions of the third layer are conducted using $v_{real}(3,i)$, the height error $e_h(3,i)$ should be measured and a new $\Delta\Delta v(4,i)$ is about to be inferred. In this way, the closed-loop control process will repeat until the whole fabrication process is completed.

According to the presented control process, the speed change applied to adjust the originally planned parameter of a bead located at the n^{th} position and the m^{th} layer is calculated as a sum of all previously inferred change increments at the same position, which can be presented as follows:

$$\Delta v(m,n) = \sum_{j=3}^{m} \Delta\Delta v(j,n) \tag{7}$$

It can be seen that the parameter adjustment is performed using the information from two sources. It considers not only the historically applied speed change in the previous layer (the deposition context) but also a newly inferred speed change increment. The output of the inference machine is indirectly applied to regulate the control process. The benefit is that fine adjustment can be achieved in cases when the height error is relatively small but a relatively big speed change is expected. Besides, the proposed solution increases the stability of control for cases that varied deposition parameters are planned for different layers. For instance, MLMB deposition may be used to fabricate components with variable widths along the vertical direction. Technical details about the design of the fuzzy-logic inference machine will be presented in the next section.

Table 1
The rule set applied by the fuzzy-logic inference machine.

$\Delta\Delta v$		Height error						
		NB	NM	NS	Z	PS	PM	PB
Error rate	NB	NB	NB	NB	NM	NM	NS	Z
	NM	NB	NB	NM	NS	NS	Z	PS
	NS	NB	NM	NS	NS	Z	PS	PM
	Z	NM	NS	NS	Z	PS	PS	PM
	PS	NM	NS	Z	PS	PS	PM	PB
	PM	NS	Z	PS	PS	PM	PB	PB
	PB	Z	PS	PM	PM	PB	PB	PB

3. Design of the fuzzy-logic inference machine

The fuzzy-logic inference machine used in this paper was implemented by the MATLAB Fuzzy Logic Toolbox. There are two inputs and one output of the fuzzy-logic inference machine. According to the application context, the universe of discourse of two inputs was specified. Since closed-loop controlling is applied layer-wise, the measured height error (unit: mm) on layer surface ranges within [−3, 3], while the range of error rate (unit: mm/layer) was assigned as [−1, 1]. The same fuzzy set with seven levels: {NB, NM, NS, Z, PS, PM, PB} were assigned to both input variables (i.e. e and Δe), and output variable (i.e. $\Delta\Delta v$).

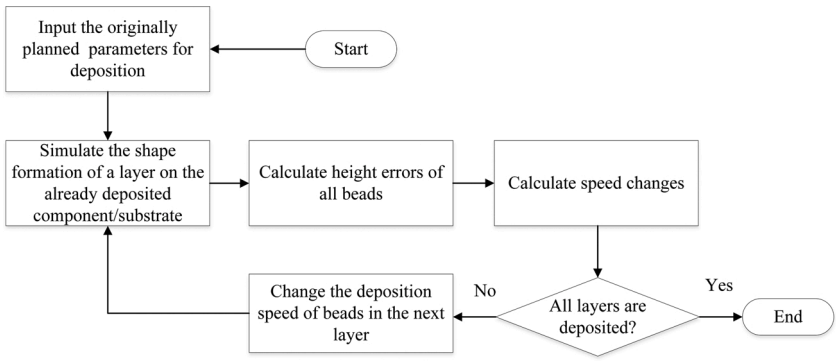

Fig. 4. The flow chart for testing the performance of the control strategy in simulation.

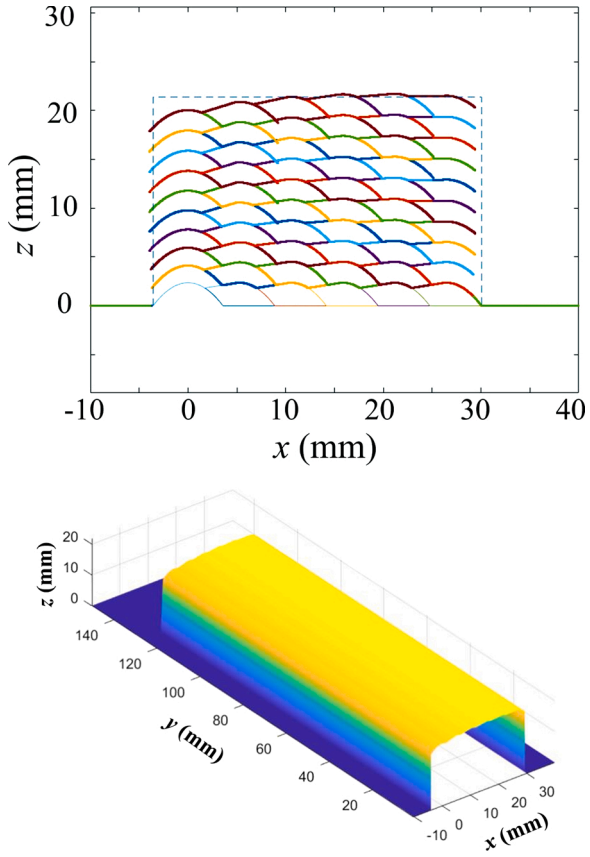

Fig. 5. A typical component virtually fabricated in simulation. a) Cross-sectional profile, b) 3D view.

Triangular shape membership functions were used to map input space to membership values, whereas the Mamdani approach was applied for inferences. Defuzzification was performed through the centroid method. After modification, the actual deposition speed (unit: mm/s) was limited within [2.5, 9]. The rule set applied for inference is shown in Table 1. Since the discourse domain of output variable (unit: mm/s^2) influences the performance of control, determination of it was performed after alternatives were designed and tested in a simulation environment.

To enable preliminarily testing the proposed control strategy and optimizing the implemented fuzzy-logic inference machine, a simulation environment was implemented, which virtually fabricate an MLMB component using a set of manufacturing parameters. The basic workflow chart of the simulation is shown in Fig. 4. The simulation started with the acquisition of parameters for fabrication of a target component, including deposition path information of all beads (i.e. 3D coordinates of the starting and ending positions of paths), and parameters applied for each deposition (i.e. wire-feeding speed, voltage and deposition speed). These parameters were carefully planned based on a BGM. Then, the forming shape of a layer was simulated, in which the cross-sectional profile of a single bead was represented by a parabola model [11], and that of multiple overlapping beads was simulated according to the principles proposed by Refs. [18,36]. In addition, to simulate the geometrical deviation of single beads caused by varying heat-dissipation fields at different positions of an MLMB component, beads in the 2nd–5th layer were set to be 1 %–4 % wider and lower comparing to their corresponding models, and beads in the 6th and above layers were set to be 5 % wider and lower.

Table 2
The parameters applied in simulation.

Parameters (Unit)	Value
Deposition speed (mm/s)	6.0
Voltage (V)	22.0
Wire feeding rate (m/min)	3.73
Width of a single bead (mm)	7.17
Height of a single bead (mm)	2.37
Step-over rate	0.738
Distance between adjacent beads in a layer (mm)	5.29
Spreading distance of lapped beads (mm)	0.33
Planned layer height (mm)	2.14

A typical component virtually fabricated in the built simulation environment is shown in Fig. 5. The component contains 10 layers, and every layer has 6 beads. Parameters presented in Table 2 were applied in the simulation without any interlayer modification. The planned layer height was calculated according to the model presented in [18]. Our previous work showed that the virtually fabricated component showed good consistency to the actual depositions. Due to the limitation of space, technical details about the simulation will not be discussed in this paper. The simulation environment was used to test the control mechanism. After a layer was deposited, the height errors of all beads in the layer were calculated. Due to the unevenness of the layer surface, the height errors were specified as the vertical distances from the planned layer surface to the shaped surface at the peak point of bead profiles. A closed-loop control mechanism was designed, in which the implemented fuzzy-logic inference machine was applied to adjust manufacturing parameters. The calculated speed changes were further applied to deposit beads in the above layer until the fabrication process finished.

Alternative discourse domains of the output variable, [−U, +U], were considered to test the performance of the implemented fuzzy-logic inference machine in simulation, to find the optimal configurations for real-life applications. To initialize the simulative testing, the following specifications were considered. The target component was a cuboid block of 30 layers. Every layer was composed of 4 beads with the deposition order from left to right. The originally planned parameters for all beads were shown in Table 2. The test considered different

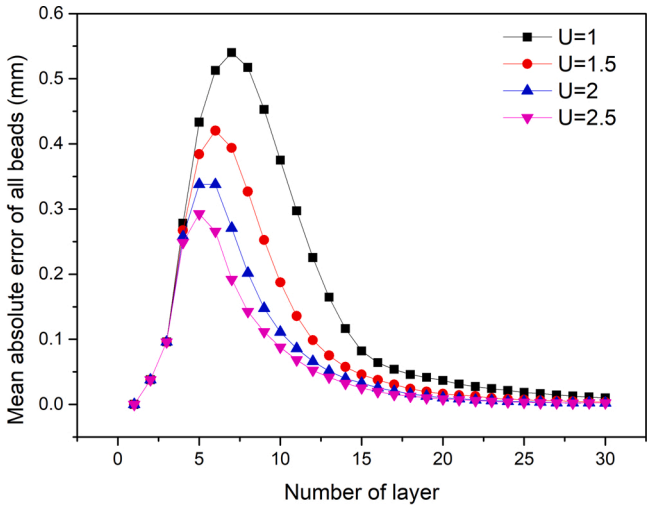

Fig. 6. The performance testing results of the fuzzy-logic inference machine with different discourse domains of output variable.

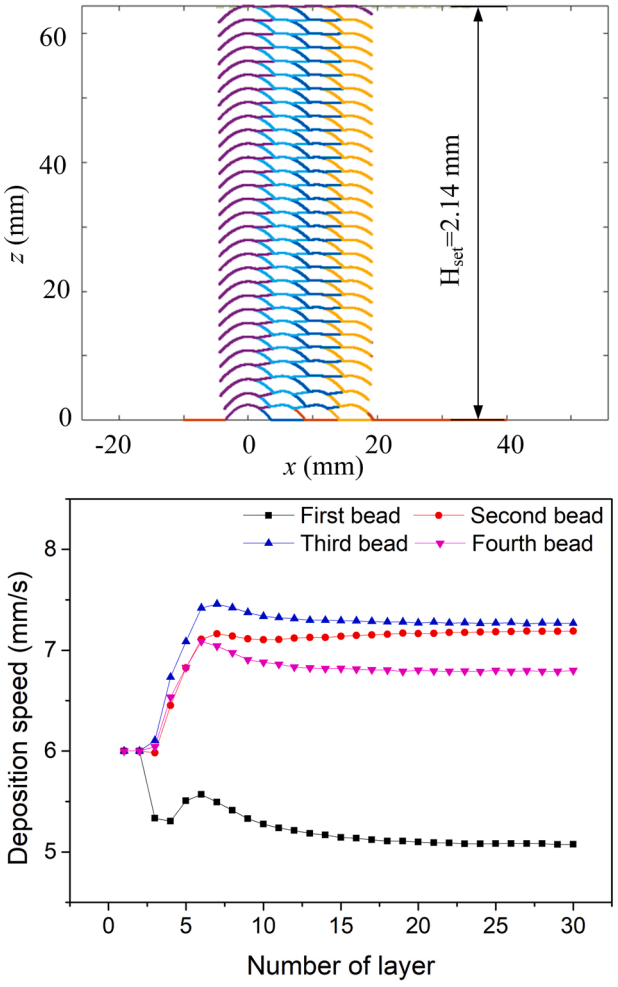

Fig. 7. The simulation result for controlling the deposition to the planned height. a) Cross-sectional profile of the component, b) Applied deposition speeds.

discourse domains ranging from 1 mm/s^2 to 2.5 mm/s^2.

The mean absolute error (MAE) of a layer was used as the indicator to evaluate the performance of control, which was calculated by the

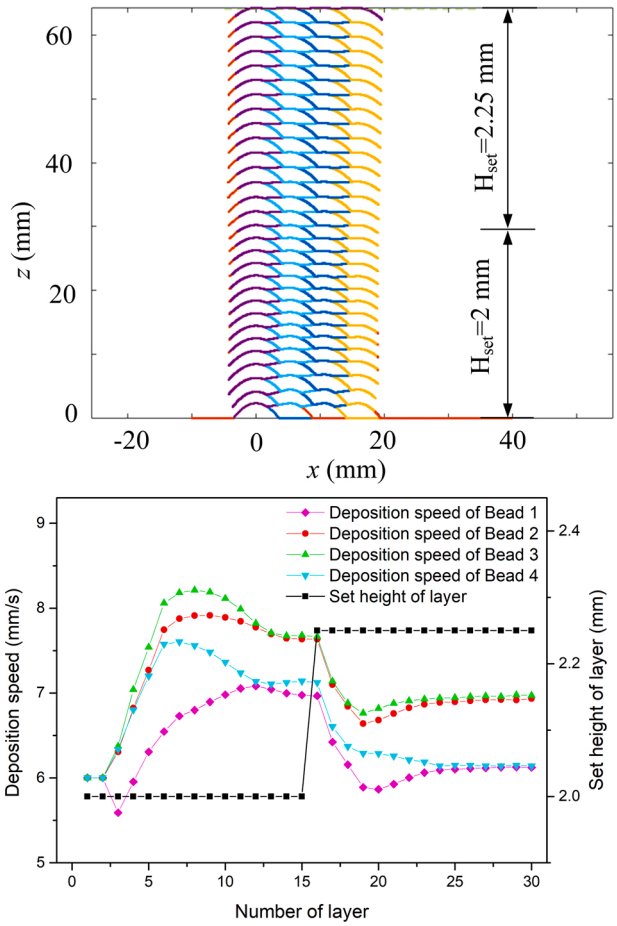

Fig. 8. The simulation result for controlling the layer height from 2 mm to 2.25 mm. a) Cross-sectional profile of the component, b) Applied deposition speeds.

following formula:

$$\mathrm{MAE}_j = \frac{1}{n}\sum_{i=1}^{n}|e(j,i)| \tag{8}$$

where MAE_j refers to the MAE of the jth layer, $e(j,i)$ refers to the height error of the ith bead in the jth layer.

The simulation results are shown in Fig. 6. It can be seen that the discourse domain of the output variable played an important role in controlling the deposition height of the MLMB component. When U is relatively small (e.g. U = 1), a large overshot can be observed, and the response experiences a long period to become stable. It implies that a small discourse domain results in a slow progression of control. The controller has a weak capability to finely adjust speed change when small deviations are observed. As a result, the controller experiences a long period of time to eliminate small errors. On the other hand, when U is relatively big (e.g. U = 2.5), the controller can respond to the error quickly, and the overshot can be reduced. However, considering the practical requirements of MLMB deposition, the formed height of a given bead depends on not only the applied deposition parameters but also the already deposited neighboring beads. A fast response may influence the beads-overlapping process. For instance, if a relatively small deposition speed is applied, the deposited bead will be so thin that a good beads-overlapping can hardly be achieved. Therefore, [−2, 2] was selected as the discourse domain of the output variable of the inference machine. In this case, the MAE of all beads in a layer was smaller than 0.1 mm after a series of adjustments were made from the 3rd layer to the 10th layer.

The simulation results of using the designed controller to regulate the

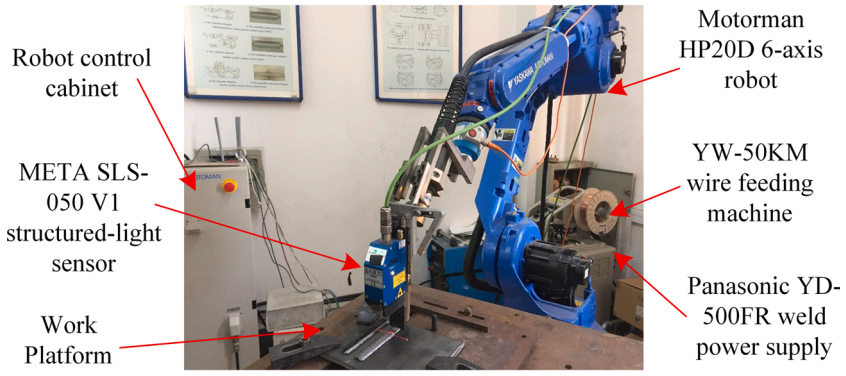

Fig. 9. Constituents of the robotic WAAM system.

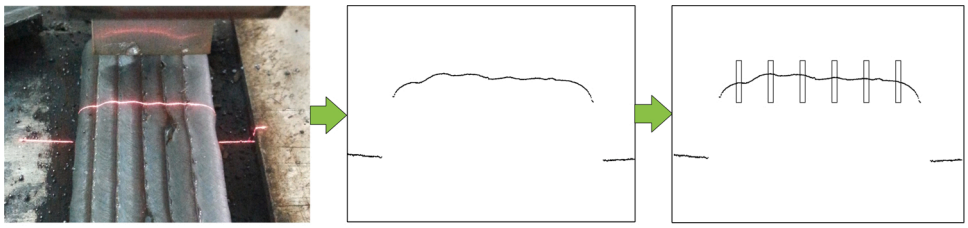

Fig. 10. The workflow for measuring the height of beads.

deposition height of the target component are shown in Fig. 7. It can be seen that layer surfaces increased steadily. The optimal deposition speeds were found at the 11th layer. The planned height of the target component was 64.11 mm. The maximum error in height on the surface of the whole component was $4*10^{-3}$ mm, which showed good height accuracy and surface flatness. In addition, the performance of the control strategy was also tested to control the layer height to a different value during the fabrication process. The second simulative test applied the parameters of Table 2 as the originally planned parameters, which aimed at fabricating layers with a height of 2.14 mm. Using the implemented controller, the following objective was set: the layer height from the 1st layer to the 15th layer should be controlled to 2 mm, while that from the 16th layer to the 30th layer should be controlled to 2.25 mm.

The simulation result of the second test is shown in Fig. 8. Two adjustment periods can be observed from the deposition speed of beads. The first adjustment period was taken to control the forming height from 2.14 mm to 2 mm. The control process went into a steady period after adjustments of 10 layers were taken. The deposition speed of beads

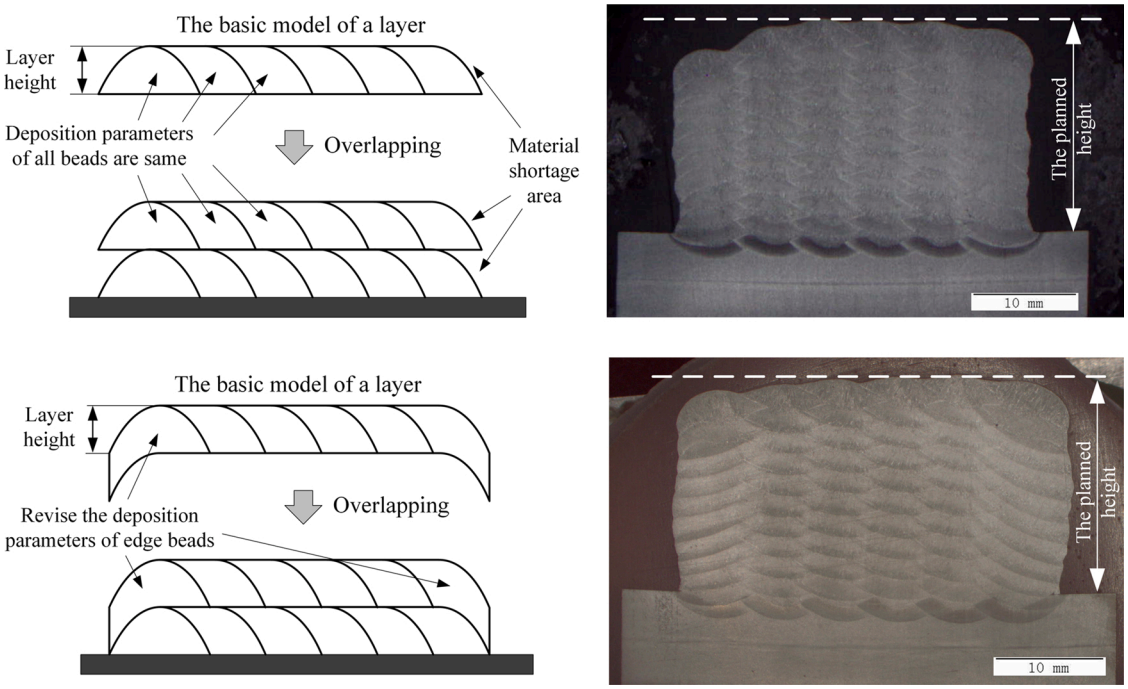

Fig. 11. The deposited components without control. a) Planned by T-LOM, b) Planned by R-LOM.

increased since the set height of layers decreased. Also, the second adjustment period controlled the forming height of beads from 2 mm to 2.25 mm. The control effort of 8 layers was spent in finding the optimal deposition speed of beads to form the given height.

As indicated by the simulation results, the designed and implemented controller showed good efficiency for controlling the deposition height of MLMB components. It can be applied for keeping the stick-out distance of deposition to a constant value in the fabrication process, which facilitates the stability of deposition. In addition, the simulation results also imply that the controller is capable to support adaptive deposition processes, such as deposition with varying layer heights. The flexibility of fabrication can be enhanced. Therefore, the effectiveness of the proposed ICLC mechanism in regulating the deposition process of WAAM is validated. Experimental testing of the performance of the proposed control mechanism in real-life cases is carried out in the next section.

4. Validation of the ICLC mechanism in real-life cases

4.1. Introducing the experimental setup

Real-life experiments were conducted based on a robotic WAAM system, which was implemented at the Harbin Institute of Technology. System constituents and arrangements are shown in Fig. 9. The accuracy of the robotic motion system was 0.06 mm. Gas metal arc welding (GMAW) was applied as the method to deposit materials on a flat substrate of Q235 steel. The feeding material for deposition was copper-coated H08Mn2Si wire with a diameter of 1.2 mm. The shielding gas was a mixture of Ar (95 %) and CO_2 (5 %), and the flow rate was set to 18 $\pm$ 0.5 L/min. A constant deposition order of beads was set to all layers. In the fabrication process, after a bead is deposited the system waited until the arc-starting position of the next bead cooled down below 50℃, preventing the deposited component from overheating.

During the interlayer idle time, the height of the deposited beads was measured by a META SLS-050 V1 linear structured-light sensor, which was attached to the weld gun. The workflow for measuring the height of beads is presented in Fig. 10. The applied sensor had a built-in image processing sub-system, which was able to aggregate the point cloud data of the light stripe with an accuracy of 0.05 mm. Since the measurements were taken in an off-line manner, the influence of arc on the projected light stripes can be avoided. The pre-processed data was delivered to the PC through Ethernet communication ten times per second, and was further used for measuring the height of beads. For every measurement, only the height of designated positions in the light stripe was considered, corresponding to the peak point of every bead profile. The height of every bead was calculated as the mean value of points locating within the range of $\pm$0.5 mm around the deposition path of the bead. After a layer was deposited, the middle part of the layer surface was scanned with a speed of 2 mm/s along the deposition direction. The total length of the cuboid block was 100 mm, and the scanned length was 60 mm. The forming height of a bead was calculated as the average measured heights reflecting its middle part, which means that the arc-starting section and arc-distinguishing section with the length of 20 mm, respectively, were excluded from the calculation.

According to the work reported in [18], two different layers-overlapping models (LOM) can be applied for determining the originally planned parameters of cuboid blocks, including the traditional layers-overlapping model (T-LOM) and the revised layers-overlapping model (R-LOM). The T-LOM considers application of the same parameters in all depositions, while R-LOM revised the deposition parameters of edge beads to compensate for material shortage areas. Therefore, parameters shown in Table 2 were applied for all depositions in the component planned by T-LOM. In the component planned by R-LOM, the deposition speed of edge beads in the second and above layers were set to 5.1 mm/s. Components having 10 layers and 6 beads in each layer were deposited using parameters planned by both LOMs without process control, which are shown in Fig. 11.

It can be seen that both components were lower than the planned height, which is indicated by the dashed lines in Fig. 11. In the component planned by T-LOM, the height error caused by the material short areas accumulated at the position of the first bead. Since beads were overlapped one after another, the height error appeared at the first bead gradually distributed to other beads, which influenced the forming height of the entire component. On the other hand, although the R-LOM was able to eliminate the height error caused by the material shortage areas, deviations on the layer surface can still be observed. They are produced owning to the accidentally collapsed materials at the lateral surfaces of the component. Therefore, a dedicated process control should be applied to ensure that the forming height of the cuboid blocks is the same as the planned value.

4.2. Testing the control strategy in fabrication of cuboid blocks

To enable validation of the proposed control strategy, a cuboid block with 15 layers*4 beads was considered as the target. According to the deposition order, beads in a layer was named as the 1st bead, the 2nd bead, the 3rd bead, and the 4th bead, respectively. The first experiment was conducted based on the parameters planned by the T-LOM. With the implemented controller, the deposition speed of beads belonging to the

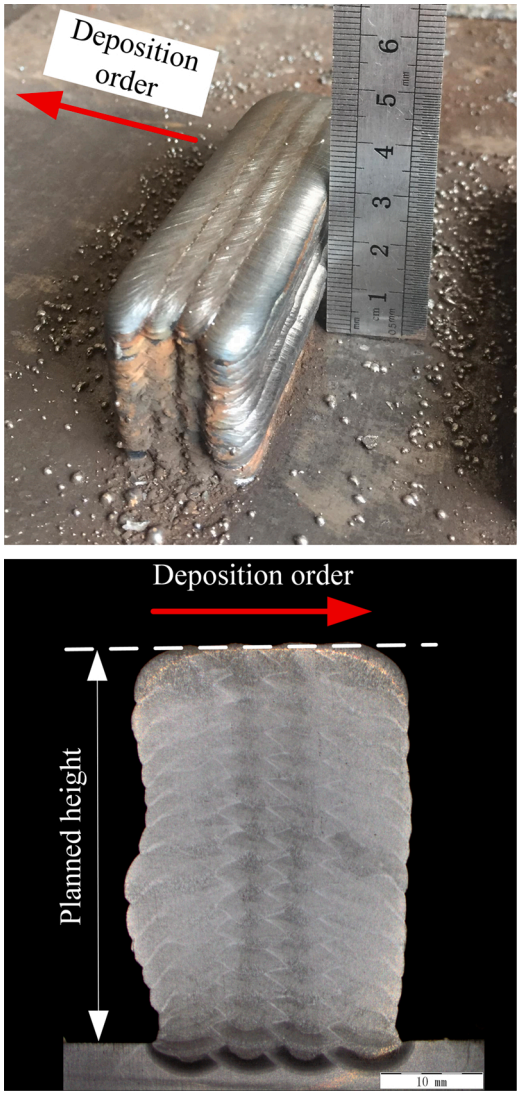

Fig. 12. The part planned based on the T-LOM and fabricated with the ICLC mechanism. a) The overall view, b) The cross-sectional profile.

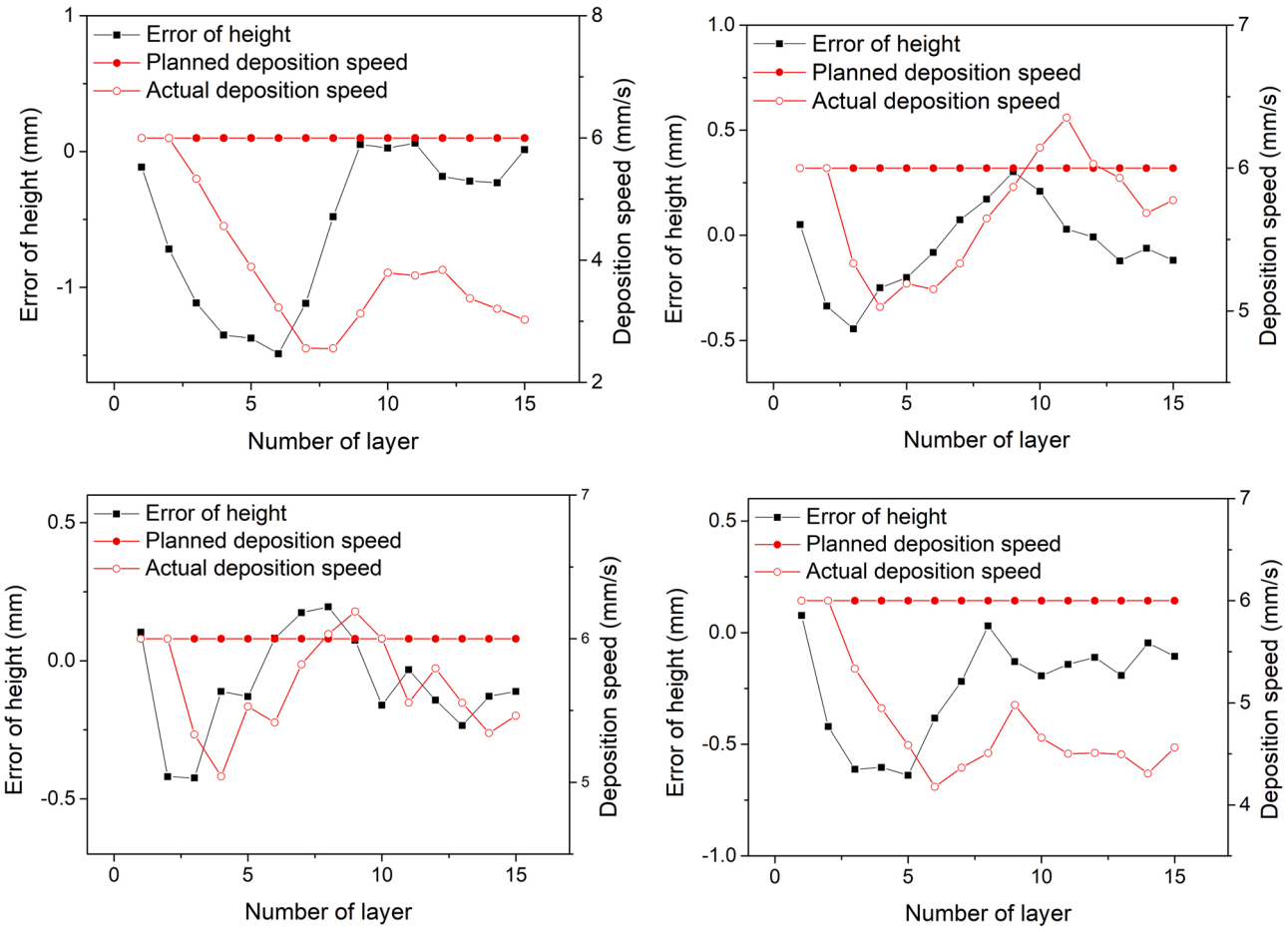

Fig. 13. The deposition speeds and height errors of beads in the part planned by T-LOM. a) The first bead of all layers, b) The second bead of all layers, c) The third bead of all layers, d) The fourth bead of all layers.

third and above layers was adjusted, while the wire-feeding speed and voltage remained the same. The fabricated component is presented in Fig. 12. The planned speed, the actual speed, and the measured height errors are shown in Fig. 13.

Since an inappropriate process model (i.e. the T-LOM) was applied in the planning phase, an instant height error was formed after the first bead in the second layer was deposited. Started from the third layer, the control aimed at minimizing the height error by reducing the deposition speed of beads. Owning to the adjustments made from the 3rd layer to the 8th layer, the height error in the first bead turned from a negative value to a positive value in the 9th layer. Then, the height error fluctuated around 0 from the 10th layer to the 15th layer. The other three beads experienced similar adaptation processes, including (i) negative height errors were observed from the 2nd layer to the 6th layer, (ii) the height error achieved zero-crossing around the 7th layer, and (iii) the height error fluctuated around zero from the 8th layer to the 15th layer. The maximum error in height of the entire component was 0.14 mm. No pore or inclusion was observed on the fabricated component, which means that a well beads-overlapping was maintained when adjustments were applied.

The experimental result implies that the proposed control mechanism can handle cases in which the T-LOM is applied to plan a cuboid component. However, due to the low speeds applied to deposit the first beads from the 3rd layer to the 9th layer, the left lateral surface appeared significant material redundancy. While the maximum error in width was 3.21 mm, the redundant material can be removed by post-machining processes to increase the fabrication accuracy of width.

The implemented control mechanism was also applied to regulate the deposition height of a cuboid component planned based on the R-LOM. When the R-LOM was applied for determining the originally planned parameters, the deposition speed of the first bead and the last bead in the second and above layers was set as 5.1 mm/s. The fabricated component is presented in Fig. 14. The planned speeds, the actual speeds, and the measured height errors are shown in Fig. 15. As shown by the experimental results, the maximum height error of the fabricated component was 0.20 mm. A steadier increase of the deposition height of all layers was achieved, comparing to the case in which the T-LOM was used. When the intentional decrease of the deposition speeds in the second layer was applied, the initial height error in the R-LOM case was smaller than that in the T-LOM case. In addition, less control effort was needed in the R-LOM case to regulate the deposition speed of the first bead from the planned value to the steady-state value (i.e. from 5.1 mm/s to 3.8 mm/s) than in the T-LOM case (i.e. from 6.0 mm/s to 3.8 mm/s). Accordingly, the material redundancy produced at the lateral surfaces was much less. The maximum error in width was reduced to 0.96 mm.

4.3. *Discussion of the results*

To plan the manufacturing parameters of a given part for WAAM, both BGM and LOM should be considered. According to the results observed from the real-life experiments, the proposed ICLC mechanism showed good adaptability in controlling the deposition height of MLMB components planned based on either the T-LOM or the R-LOM. In the case that R-LOM and the ICLC mechanism were jointly applied, the deposited MLMB component had good geometrical accuracy in both height and width. For this reason, a well-defined BGM and a proper LOM (e.g. the R-LOM) are still the most crucial fundamentals for MLMB deposition, which have been seen as the preconditions of the proposed

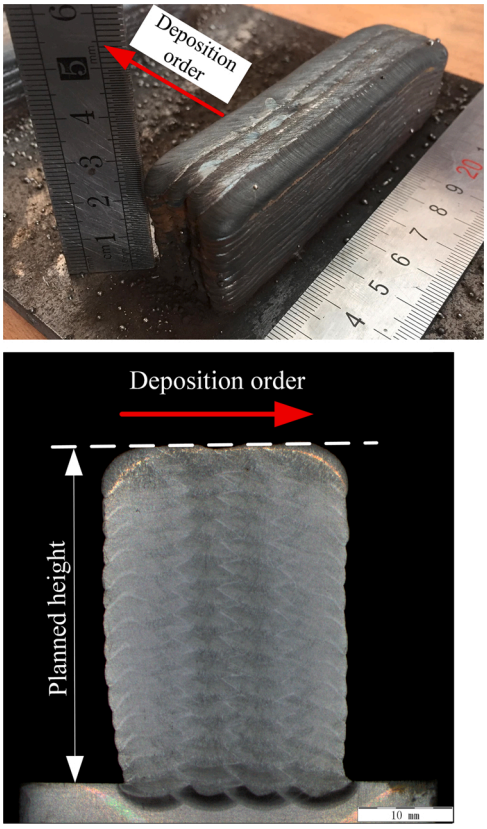

Fig. 14. The part planned based on the R-LOM and fabricated with the ICLC mechanism. a) The overall view, b) The cross-sectional profile.

mechanism.

Concerning the designed fuzzy-logic inference machine, the deposition speed was the only factor used to adjust the forming height. However, the bead width also changes positively to the change of the deposition speed. On the one hand, a changed deposition speed may produce material redundancy on the lateral surface, as shown in the experimental results. It also influences the overlapping of beads. This is because that the proposed control mechanism considers changing deposition parameters rather than deposition paths. Both parameters and paths are jointly determined in the process planning phase based on a given step-over rate. As a consequence, if a deposited bead is thinner than its planned model, then a rough overlapping may happen. The heat-sink effect of WAAM reduces the solidification speed of weld pool, which improves the quality of beads-overlapping in high layers. This is the main reason why a good combination quality of beads was achieved in the components with varying deposition speeds. On the other hand, if a bead is wider than the planned model, then its neighboring beads will be propped up. The implication is that although beads at different positions of a layer are controlled by independent sub-controllers, their forming processes are interrelated. An error that appeared at a bead may produce responses to all sub-controllers. Therefore, the steady-state of the entire control process should be the situation that all sub-controllers become settled.

Another important observation is that the ICLC mechanism is flexible, general and hysteresis-free. Firstly, this approach can be applied from any layer of a part in its fabrication process. The only constraint is that adjustment of deposition parameters can be applied after the surface information of two successive layers is aggregated. In addition, the proposed approach does not need an accurate process model to infer parameter adjustments. It can also be adapted to other metal AM approaches for dimensional control, such as laser deposition or electron beam deposition. Furthermore, the ICLC approach applies an instant response whenever an error is observed, and the effect of response can be immediately observed after the adjustment is made. Therefore, this approach provides a practical solution to deal with interlayer observed geometrical issues and prevent the issues from getting worse. The practical value of the developed approach is multifold. It not only decreased the amount of material redundancy and increased the material utilization rate, but also improved process stability of deposition. Especially, the proposed approach facilitates fabrication of large-scale metal parts from CAD models to finished parts in a fully automatic manner.

5. Conclusions and future work

A novel control mechanism for enhancing the fabrication accuracy of multi-layer multi-bead (MLMB) components by wire and arc additive manufacturing (WAAM) is proposed in this paper. It considers the geometrical errors measured on already deposited layers to adjust deposition parameters of beads in the subsequent layers, forming an interlayer closed-loop control (ICLC) mechanism. Fundamentals of the control mechanism were discussed and technical details about a fuzzy logic inference machine were presented. Confirmative experiments were conducted to investigate the performance of the implemented controller. According to the conducted work, conclusions can be drawn as follows:

- The proposed ICLC mechanism is an effective approach for controlling the forming height of cuboid steel blocks deposited by wire and arc additive manufacturing. In the conducted experiments, the height error of cuboid blocks was limited within 0.20 mm.
- The height control approach proposed in the paper employs multiple sub-controllers to individually govern the forming height of beads, which enables considering the deposition context of beads for parameter adjustment. Every sub-controller inherits the historically applied change as a vertical deposition context, which enhances the stability of control when a small error is observed.
- The ICLC mechanism is very sensitive to the correctness of planned deposition parameters. Integrative utilization of the revised layers-overlapping model (R-LOM) and the ICLC mechanism to fabricate cuboid components can eliminate width fluctuations.

The work presented in this paper showed several limitations, which provide many opportunities for further investigations. Firstly, this paper demonstrates the effectiveness of the ICLC mechanism by applying it to control the forming height of cuboid components. A width control approach will be carried out to adjust the deposition parameters of edge beads to control both width and height. Besides, this paper employs a fuzzy-logic inference machine as the basis for control. The correlations between deposition parameters and horizontal context (e.g. geometries of the neighboring bead) as the inputs, and the respond of bead geometry change as the output should be further investigated to enable a more effective control, such as application of model-based predictive control method. Furthermore, the developed height control approach is dedicated to the fabrication of cuboid parts. The approach should be adapted to more complex structures, such as a funnel-shaped structure, in which the number of beads between two successive layers is different. Last but not the least, the height measurement method applied in this study is only appropriate for simple cases, e.g. straight and parallelly arranged paths. A general and effective sensing method for layer surface

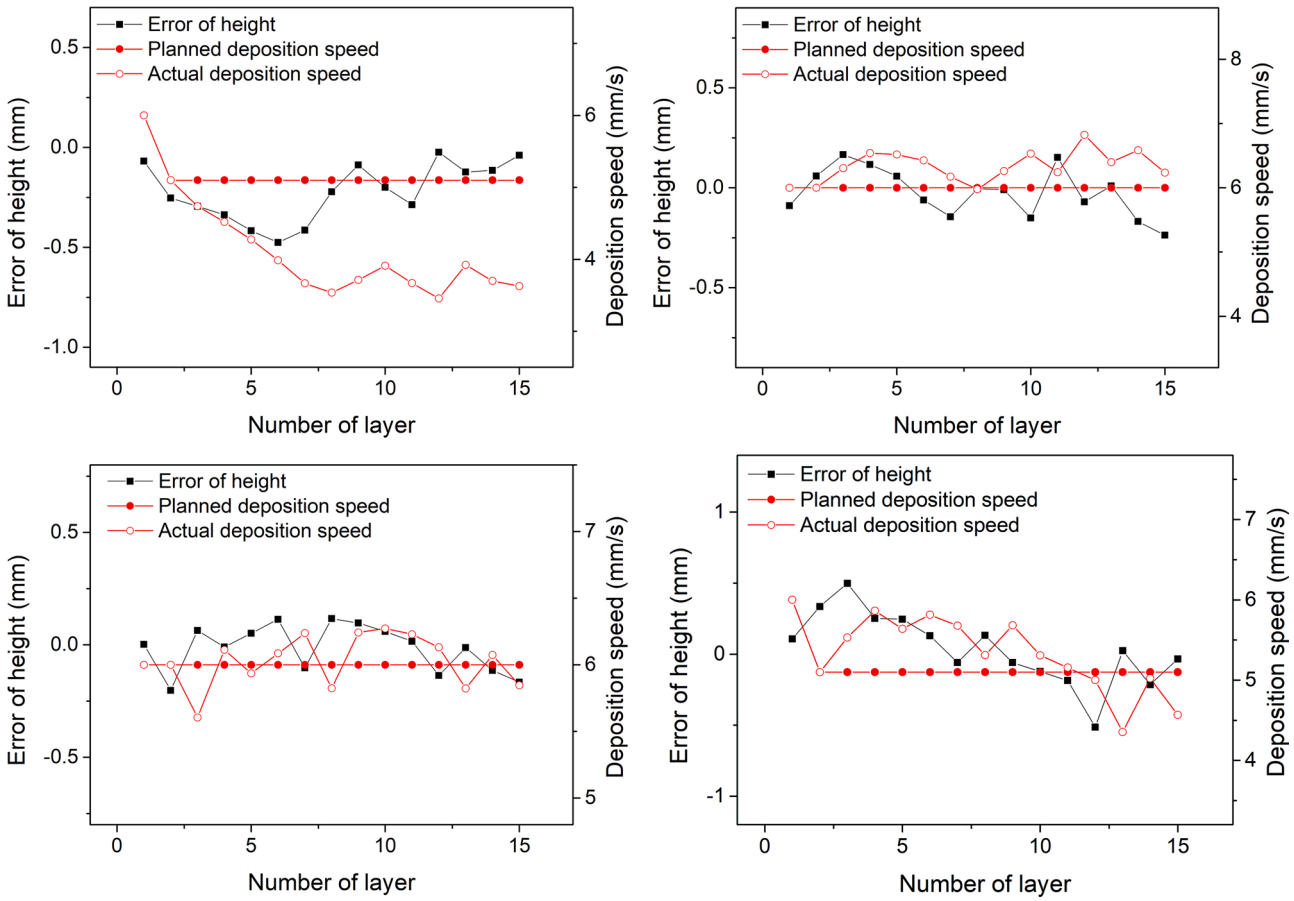

Fig. 15. The deposition speed and height error of beads in the part planned with R-LOM. a) The first bead of all layers, b) The second bead of all layers, c) The third bead of all layers, d) The fourth bead of all layers.

measurement for complex cases should be focused in future work, e.g. curved structure, 3D-surface.

Author's contribution

Dr. Yongzhe Li conceived the theory, designed experiments and wrote the paper. Xinlei Li contributed to the implementation work. Prof. Guangjun Zhang initialized and supervised the research. Prof. Imre Horváth contributed to the conceptualization work. Qinglin Han helped with the experiments.

Declaration of Competing Interest

The authors declare that they have no known competing financial interests or personal relationships that could have appeared to influence the work reported in this paper.

Acknowledgment

This work was supported by Key R&D Project of Guangdong Province, China (2018B090906004) and the National Key R&D Program of China (2018YFB1105800).

References

[1] Williams S, Martina F, Addison AC, Ding J, Pardal G, Colegrove P. Wire + arc additive manufacturing. Mater Sci Technol 2016;32:641–7. https://doi.org/10.1179/1743284715Y.0000000073.

[2] Wu B, Pan Z, Ding D, Cuiuri D, Li H, Xu J, et al. A review of the wire arc additive manufacturing of metals: properties, defects and quality improvement. J Manuf Process 2018;35:127–39. https://doi.org/10.1016/j.jmapro.2018.08.001.

[3] Gokuldoss PK, Kolla S, Eckert J. Additive manufacturing processes: selective laser melting, electron beam melting and binder jetting-selection guidelines. Materials 2017;10:672. https://doi.org/10.3390/ma10060672.

[4] Murr LE, Gaytan SM, Ramirez DA, Martinez E, Hernandez J, Amato KN, et al. Metal fabrication by additive manufacturing using laser and electron beam melting technologies. J Mater Sci Technol 2012;28:1–14. https://doi.org/10.1016/S1005-0302(12)60016-4.

[5] Rodrigues TA, Duarte V, Miranda RM, Santos TG, Oliveira JP. Current status and perspectives on wire and arc additive manufacturing (WAAM). Materials 2019;12:1121. https://doi.org/10.3390/ma12071121.

[6] Frazier WE. Metal additive manufacturing: a review. J Mater Eng Perform 2014;23:1917–28. https://doi.org/10.1007/s11665-014-0958-z.

[7] Zhang Y, Chen Y, Li P, Male AT. Weld deposition-based rapid prototyping: a preliminary study. J Mater Process Technol 2003;135:347–57. https://doi.org/10.1016/S0924-0136(02)00867-1.

[8] Qi Z, Qi B, Cong B, Sun H, Zhao G, Ding J. Microstructure and mechanical properties of wire + arc additively manufactured 2024 aluminum alloy components: as-deposited and post heat-treated. J Manuf Process 2019;40:27–36. https://doi.org/10.1016/j.jmapro.2019.03.003.

[9] Abe T, Sasahara H. Layer geometry control for the fabrication of lattice structures by wire and arc additive manufacturing. Addit Manuf 2019;28:639–48. https://doi.org/10.1016/j.addma.2019.06.01.

[10] Li R, Xiong J, Lei Y. Investigation on thermal stress evolution induced by wire and arc additive manufacturing for circular thin-walled parts. J Manuf Process 2019;40:59–67. https://doi.org/10.1016/j.jmapro.2019.03.006.

[11] Ding D, Pan Z, Cuiuri D, Li H. A multi-bead overlapping model for robotic wire and arc additive manufacturing (WAAM). Robot Comput Integr Manuf 2015;31:101–10. https://doi.org/10.1016/j.rcim.2014.08.008.

[12] Ding D, Pan Z, Cuiuri D, Li H. Wire-feed additive manufacturing of metal components: technologies, developments and future interests. Int J Adv Manuf Tech 2015;81:465–81. https://doi.org/10.1007/s00170-015-7077-3.

[13] Xiong J, Zhang G, Hu J, Wu L. Bead geometry prediction for robotic GMAW-based rapid manufacturing through a neural network and a second-order regression analysis. J Intell Manuf 2014;25:157–63. https://doi.org/10.1007/s10845-012-0682-1.

[14] Ding D, Pan Z, Cuiuri D, Li H, Van Duin S, Larkin N. Bead modelling and implementation of adaptive MAT path in wire and arc additive manufacturing. Robot Comput Integr Manuf 2016;39:32–42. https://doi.org/10.1016/j.rcim.2015.12.004.

[15] Panda B, Shankhwar K, Garg A, Savalani MM. Evaluation of genetic programming-based models for simulating bead dimensions in wire and arc additive manufacturing. J Intell Manuf 2019;30:809–20. https://doi.org/10.1007/s10845-016-1282-2.
[16] Geng H, Xiong J, Huang D, Lin X, Li J. A prediction model of layer geometrical size in wire and arc additive manufacture using response surface methodology. Int J Adv Manuf Tech 2017;93:175–86. https://doi.org/10.1007/s00170-015-8147-2.
[17] Xiong J, Zhang G, Hu J, Li Y. Forecasting process parameters for GMAW-based rapid manufacturing using closed-loop iteration based on neural network. Int J Adv Manuf Tech 2013;69:743–51. https://doi.org/10.1007/s00170-013-5038-2.
[18] Li Y, Han Q, Zhang G, Horváth I. A layers-overlapping strategy for robotic wire and arc additive manufacturing of multi-layer multi-bead components with homogeneous layers. Int J Adv Manuf Tech 2018;96:3331–44. https://doi.org/10.1007/s00170-018-1786-3.
[19] Li Y, Huang X, Horváth I, Zhang G. GMAW-based additive manufacturing of inclined multi-layer multi-bead parts with flat-position deposition. J Mater Process Technol 2018;262:359–71. https://doi.org/10.1016/j.jmatprotec.2018.07.010.
[20] Li Y, Han Q, Horváth I, Zhang G. Repairing surface defects of metal parts by groove machining and wire + arc based filling. J Mater Process Technol 2019;274:116268. https://doi.org/10.1016/j.jmatprotec.2019.116268.
[21] Thapliyal S. Challenges associated with the wire arc additive manufacturing (WAAM) of aluminum alloys. Mater Res Express 2019;6:11. https://doi.org/10.1088/2053-1591/ab4dd4.
[22] Xiong J, Liu G, Pi Y. Increasing stability in robotic GTA-based additive manufacturing through optical measurement and feedback control. Robot Comput Integr Manuf 2019;59:385–93. https://doi.org/10.1016/j.rcim.2019.05.012.
[23] Xiong J, Zhang G, Qiu Z, Li Y. Vision-sensing and bead width control of a single-bead multi-layer part: material and energy savings in GMAW-based rapid manufacturing. J Clean Prod 2013;41:82–8. https://doi.org/10.1016/j.jclepro.2012.10.009.
[24] Xiong J, Yin Z, Zhang W. Closed-loop control of variable layer width for thin-walled parts in wire and arc additive manufacturing. J Mater Process Technol 2016;233:100–6. https://doi.org/10.1016/j.jmatprotec.2016.02.021.
[25] Xiong J, Zhang G. Adaptive control of deposited height in GMAW-based layer additive manufacturing. J Mater Process Technol 2014;214:962–8. https://doi.org/10.1016/j.jmatprotec.2013.11.014.
[26] Honnige JR, Colegrove PA, Ganguly S, Eimer E, Kabra S, Williams S. Control of residual stress and distortion in aluminium wire plus arc additive manufacture with rolling. Addit Manuf 2018;22:775–83. https://doi.org/10.1016/j.addma.2018.06.015.
[27] Li F, Chen S, Shi J, Zhao Y. In-process control of distortion in wire and arc additive manufacturing based on a flexible multi-point support fixture. Sci Technol Weld Joi 2019;24:36–42. https://doi.org/10.1080/13621718.2018.1476083.
[28] Li F, Chen S, Wu Z, Yan Z. Adaptive process control of wire and arc additive manufacturing for fabricating complex-shaped components. Int J Adv Manuf Tech 2018;96:871–9. https://doi.org/10.1007/s00170-018-1590-0.
[29] Xu B, Tan X, Gu X, Ding D, Deng Y, Chen Z, et al. Shape-driven control of layer height in robotic wire and arc additive manufacturing. Rapid Prototyp J 2019;25:1637–46. https://doi.org/10.1108/RPJ-11-2018-0295.
[30] Radel S, Diourte A, Soulie F, Company O, Bordreuil C. Skeleton arc additive manufacturing with closed loop control. Addit Manuf 2019;26:106–16. https://doi.org/10.1016/j.addma.2019.01.003.
[31] Radel S, Bordreuil C, Soulié F, Company O. CAM for on-line control for wire arc additive manufacturing. Comput Aided Des Appl 2019;16:558–69. https://doi.org/10.14733/cadaps.2019.558-569.
[32] Xiong J, Lei Y, Chen H, Zhang G. Fabrication of inclined thin-walled parts in multi-layer single-pass GMAW-based additive manufacturing with flat position deposition. J Mater Process Technol 2017;240:397–403. https://doi.org/10.1016/j.jmatprotec.2016.10.019.
[33] Ji L, Lu J, Tang S, Wu Q, Wang J, Ma S, et al. Research on mechanisms and controlling methods of macro defects in TC4 alloy fabricated by wire additive manufacturing. Materials 2018;11:1104. https://doi.org/10.3390/ma11071104.
[34] Han Q, Li Y, Zhang G. Online control of deposited geometry of multi-layer multi-bead structure for wire and arc additive manufacturing. In: Chen S, Zhang Y, Feng Z, editors. Transactions on intelligent welding manufacturing. Singapore: Springer; 2018. p. 85–93. https://doi.org/10.1007/978-981-10-5355-9_7.
[35] Ugla A, Yilmaz O, Almusawi A. Development and control of shaped metal deposition process using tungsten inert gas arc heat source in additive layered manufacturing. Proc IMechE Part B: J Eng Manuf 2018;232:1628–41. https://doi.org/10.1177/0954405416673112.
[36] Li Y, Sun Y, Han Q, Zhang G, Horváth I. Enhanced beads overlapping model for wire and arc additive manufacturing of multi-layer multi-bead metallic parts. J Mater Process Technol 2018;252:838–48. https://doi.org/10.1016/j.jmatprotec.2017.10.017.
[37] Liu Y, Zhang Y. Model-based predictive control of weld penetration in gas tungsten arc welding. IEEE Trans Control Syst Technol 2014;22:955–66. https://doi.org/10.1109/TCST.2013.2266662.
[38] Taysom B, Sorensen C, Hedengren J. Dynamic modeling of friction stir welding for model predictive control. J Manuf Process 2016;23:165–74. https://doi.org/10.1016/j.jmapro.2016.06.004.
[39] Chen F, Xiang J, Thomas D, Murphy A. Model-based parameter optimization for arc welding process simulation. Appl Math Model 2020;81:386–400. https://doi.org/10.1016/j.apm.2019.12.014.
[40] Liu Y, Zhang Y. Iterative local ANFIS-based human welder intelligence modeling and control in pipe GTAW process: a data-driven approach. IEEE ASME Trans Mechatron 2015;20:1079–88. https://doi.org/10.1109/TMECH.2014.2363050.
[41] Zadeh LA. Fuzzy sets. Inf Control 1965;8:338–53. https://doi.org/10.1016/S0019-9958(65)90241-X.
[42] Di L, Srikanthan T, Chandel R, Katsunori I. Neural-network-based self-organized fuzzy logic control for arc welding. Eng Appl Artif Intell 2001;14:115–24. https://doi.org/10.1016/S0952-1976(00)00057-9.
[43] Liu Y, Zhang W, Zhang Y. Dynamic neuro-fuzzy-based human intelligence modeling and control in GTAW. IEEE Trans Autom Sci Eng 2015;12:324–35. https://doi.org/10.1109/TASE.2013.2279157.
[44] Podržaj P, Simončič S. Resistance spot welding control based on fuzzy logic. Int J Adv Manuf Tech 2011;52:959–67. https://doi.org/10.1007/s00170-010-2794-0.
[45] Heidarzadeh A, Testik Ö, Güleryüz G, Barenji R. Development of a fuzzy logic based model to elucidate the effect of FSW parameters on the ultimate tensile strength and elongation of pure copper joints. J Manuf Process 2020;53:250–9. https://doi.org/10.1016/j.jmapro.2020.02.020.
[46] Hua Y, Choi J. Adaptive direct metal/material deposition process using a fuzzy logic-based controller. J Laser Appl 2005;17:200–10. https://doi.org/10.2351/1.2098811.
[47] Xiong J, Shi M, Liu Y, Yin Z. Virtual binocular vision sensing and control of molten pool width for gas metal arc additive manufactured thin-walled components. Addit Manuf 2020;33:101121.

Dr. Yongzhe Li earned his first Ph.D. in Materials Processing Engineering at the Harbin Institute of Technology. He also holds a Ph.D. degree in Design Engineering obtained from the Delft University of Technology. His current research interests include wire and arc additive manufacturing, weld process monitoring and control, smart cyber-physical systems, dynamic context information management.

Xinlei Li is a Ph.D. candidate at the State Key Laboratory of Advanced Welding and Joining of Harbin Institute of Technology. His current research interests are robotic manufacturing, laser scanning, sensor calibration algorithms.

Prof. Guangjun Zhang is a full professor at the State Key Laboratory of Advanced Welding and Joining of the Harbin Institute of Technology. He obtained his doctoral degree from the Harbin Institute of Technology in 2002. His research interest includes robotic and intelligent welding, weld based additive manufacturing and arc welding process control.

Prof. Imre Horváth is a chair professor at the Faculty of Industrial Design Engineering, Delft University of Technology. He is the initiator of the TMCE Symposia. He served on the Executive Board of the CIE Division of ASME and is now a fellow of ASME. He is the emeritus editor of Journal CAD and associate editor of the Journal of Engineering Design. His current research interest is cognitive engineering of smart cyber-physical systems.

Qinglin Hanis a Ph.D.student at the School of Materials Science and Engineering of the Harbin Institute of Technology. He received his master's degree from the Harbin Institute of Technology in 2016. His current research interests are metal 3D printing, twin electrode gas tungsten arc deposition, gradient materials fabrication, weld process control.